Eur. Phys. J. C (2022) 82:770
https://doi.org/10.1140/epjc/s10052-022-10729-8

THE EUROPEAN PHYSICAL JOURNAL C

Regular Article - Theoretical Physics

Thermodynamics of the Reissner–Nordström-de Sitter spacetime with quintessence

Yang Zhang, Yu-Bo Ma, Yun-Zhi Du[a], Huai-Fan Li[b], Li-Chun Zhang

Institute of Theoretical Physics, Shanxi Datong University, Datong 037009, China

Received: 12 April 2022 / Accepted: 18 August 2022 / Published online: 1 September 2022

Abstract For Anti-de Sitte (AdS) black holes, the isochoric heat capacity of system is vanished, while the isobaric heat capacity is not. However, this situation does not hold on for de Sitter (dS) black holes. In this work, by introducing the interaction between the black hole horizon and the cosmological horizon of the Reissner–Nordström-de Sitter (RNdS) spacetime with quintessence, we discuss the phase transition of this system. The results show that the spacetime not only has the similar phase transition behavior to that of Van der Waals (VdW) system, and the non-vanishing isochoric heat capacity fulfills the whole thermodynamics system. Through the discussion of the entropic force between two horizons, we find out the role of entropic force in the evolution of spacetime. In addition, we also study the influence of various parameters on the phase transition and entropic force, which will provide a new method for exploring the interaction among black hole molecules from a micro perspective.

1 Introduction

As is well known, a black hole is a celestial body whose gravity is so strong that even light cannot escape. Recently, the cooperation groups of LIGO and Virgo have repeatedly observed gravitational wave signals from double black hole merging events, and the cooperation group of EHT photographed the shadow of the supermassive black hole in the center of the $M87$ elliptical galaxy [1–7]. These are observational evidence of the strong gravitational effect of black holes. In fact, a black hole is not only a strong gravitational system, but also a thermodynamic system. As early as 1970s, physicists such as Hawking and Bekenstein have established the four laws of black hole thermodynamics [8–11].

In order to explore the microstructure and evolution of black holes, people regard the cosmological constant of n-dimensional AdS spacetime as the state parameter of the black hole thermodynamic system – pressure [12]

$$P = \frac{n(n-1)}{16\pi l^2},\ \Lambda = -\frac{n(n-1)}{2l^2}, \tag{1.1}$$

where the parameter l stands for the curvature radius of the AdS spacetime. The corresponding conjugate thermodynamic quantity is the volume

$$V = \left(\frac{\partial M}{\partial P}\right)_{S,Q_i,J_k}, \tag{1.2}$$

where Q_i and J_k are the charge parameter and the angular momentum parameter, respectively. Based on this issue, a series of studies on the thermodynamic behavior of AdS black holes have been done in the extended phase space [13–31]. Firstly, people found that the charged AdS black hole has a behavior similar to Van de Waals phase transition when choosing the quantities P and V as the independent dual variables. Subsequently, it has been proved in Ref. [32] that a charged AdS black hole possesses the Van der Waals (VdW) phase transition behavior by choosing $Q^2 - \Psi$ as the independent dual variables. These developments of AdS black hole thermodynamic properties will not only help us understand the nature of black holes, but also help us to explore the microstructure of black holes [33–42].

In addition, since our universe during the inflationary period was a quasi-de Sitter spacetime, that drives our attention to a dS spacetime. Considering the cosmological constant in a dS spacetime as the dark energy, our accelerated expanding universe will evolve into a new de Sitter phase in the future [43]. Therefore, we should pay more attention on the relation between the classical, quantum, and thermodynamic properties of dS spacetime. While there are merely works on the thermodynamic behavior of black holes in a dS spacetime [44–58], the related thermodynamic properties of dS black holes will help us understand the relation between gravity and the conformal field theory. However, the investigation of the black hole thermodynamic proper-

[a] e-mail: duyzh22@sxdtdx.edu.cn (corresponding author)
[b] e-mail: huaifan999@163.com

ties in a dS spacetime is a complicated problem, since the absence of an everywhere timelike Killing vector outside the black hole horizon leads to an unclear definition of asymptotic mass. Furthermore, in a dS spacetime the black hole and cosmological horizons yield two distinct temperatures, which suggests that the system is in a non-equilibrium state.

The authors in Ref. [59] had shown that when the interaction between the black hole and cosmological horizons of the Reissner–Nordström-de Sitter black hole surrounded by quintessence (RN-dSQ) is considered, the entropy is the summation of the corresponding entropy for two horizons, and together with their interaction term, i.e.

$$S = S_c(1 + x^2 + f(x)), \tag{1.3}$$

where S_c is the entropy of cosmological horizon and x is ratio of positions of two horizons and the interaction term reads

$$f(x) = \frac{8}{5}(1 - x^3)^{2/3} - \frac{2(4 - 5x^3 - x^5)}{5(1 - x^3)}. \tag{1.4}$$

The corresponding effective temperature satisfies $T_{eff} = T_+ = T_c$, when the two horizon temperatures are equal. This result fulfills the requirements of ordinary thermodynamic systems. Therefore, the effective thermodynamic quantities of a dS spacetime are more general after considering the interaction between two horizons. Their results have been shown that this system also has a continuous phase transition similar to the Van de Waals system or a charged AdS black hole, and parameters of this system influence the phase transition. However, a vanishing isochoric heat capacity in this case is unacceptable, which has aroused people's attention [60,61]. When the effective thermodynamic quantities are used to describe the thermodynamic properties of spacetime, the isochoric heat capacity will not vanish. In this sense, under the consideration of interaction between two horizons, the method of the effective thermodynamic quantities to describe the thermodynamic properties of de Sitter spacetime has a more universal physical meaning. Furthermore, from the total entropy between two horizons in a RN-dSQ spacetime, the entropic force in the evolution of a dS spacetime plays a significant role, which presents a new approach for studying the interaction of microscopic particles inside black holes and simulating the evolution of our accelerated universe.

This article is organized as follows. In Sect. 2, we discuss the conditions for the existence of black hole and cosmological horizons in RN-dSQ spacetime, as well as the influence of spacetime parameters, and give the range of the position ratio x of two horizons. In Sect. 3, we present the effective thermodynamic quantities of RN-dSQ spacetime, and analyse the relation between the effective temperature T_{eff} and the position ratio x of two horizons. The merely consistency between the effective temperature and black hole horizon temperature reminds us that when studying the spacetime thermodynamic properties of RN-dSQ, replacing the effective temperature T_{eff} with the black hole horizon radiation temperature T can simplify the problem. In Sect. 4, we extend the method of the phase transition for Van de Waals systems or charged AdS black holes, and use it to study the RN-dSQ spacetime, and obtain the phase transition properties of the RN-dSQ spacetime. In Sect. 5, we explore the entropic force between two horizons of the RN-dSQ spacetime, and obtain the function of entropic force with respect to position ratio x. It is found that the law of entropic force changing with x is very similar to the Lennard–Jones force between two microscopic particles. This phenomenon provides a new way for us to further study the interaction of black hole molecules. The Sect. 6 is the summary.

2 Reissner–Nordström-de Sitter black hole surrounded by quintessence

When solving the Einstein–Maxwell field equation with the cosmological constant, in 2003 Kiselev considered the quintessence dark energy [62]

$$T_t^t = T_r^r = \rho_q + \frac{\alpha}{r^2}, \tag{2.1}$$

$$T_\theta^\theta = T_\varphi^\varphi = -\frac{1}{2}\rho_q(3\omega + 1), \tag{2.2}$$

where $\rho_q = -\frac{3\alpha\omega}{2r^{3(\omega+1)}}$ is the density of quintessence field, ω $(-1 < \omega < -1/3)$ is the quintessence dark energy barotropic index, α is the normalization factor associated with the quintessence density of dark energy and is always positive. On this issue, the static spherically symmetric solution of Einstein–Maxwell field equation for a Reissner–Nordström-dS (RN-dS) black hole in quintessence matters had been given by Refs. [59,63]

$$ds^2 = -g(r)dt^2 + g^{-1}dr^2 + r^2 d\Omega_2^2 \tag{2.3}$$

with the metric function

$$g(r) = 1 - \frac{2M}{r} + \frac{Q^2}{r^2} - \frac{r^2}{l^2} - \alpha r^{-3\omega-1}. \tag{2.4}$$

Here M and Q represent the black hole mass and charge, l is the curvature radius of a pure dS spacetime.

Now, let us analyze the existence of black hole and cosmological horizons, which are determined by the following equation

$$1 - \frac{2M}{r} + \frac{Q^2}{r^2} - \frac{r^2}{l^2} - \alpha r^{-3\omega-1} = 0. \tag{2.5}$$

Solving Eq. (2.5), one can obtain

$$M = \frac{r}{2}\left(1 + \frac{Q^2}{r^2} - \frac{r^2}{l^2} - \alpha r^{-3\omega-1}\right). \tag{2.6}$$

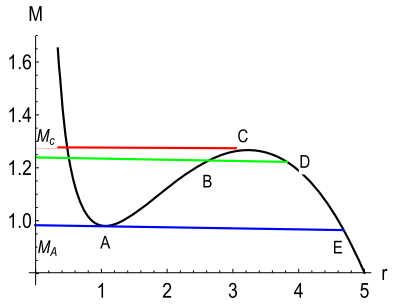

Fig. 1 $M-r$ diagram for $Q=1, \alpha=0.01, \omega=-2/3, l^2=37.386$

By choosing $Q=1, \omega=-2/3, l^2=37.386, \alpha=0.01$, the $M-r$ curve is shown in Fig. 1. Note that the curvature radius of dS spacetime should be big than the black hole event horizon, here we set it to $l\sim 6$. It can be seen from the $M-r$ graph that there exist the local stable minimum and unstable maximum, which are denoted by the uppercase letters A and C. The corresponding mass parameters are M_A and M_C. As $M_A<M<M_C$, the RN-dSQ spacetime possesses possibly the black hole interior horizon r_-, the black hole event horizon r_+ (i.e., black hole horizon in the following), and the cosmological horizon r_c. At the point C, the black hole horizon coincides with the cosmological one, and this point also corresponds to the maximum energy of the black hole $M=M_C$. At the point A, the interior and event horizons of black hole coincide, and it is also the lowest limit of the smallest black hole $M=M_A$. Black hole does not exist in RN-dSQ spacetime when $M>M_C$ or $M<M_A$ [64]. In order to study the thermodynamic properties of a dS spacetime endowed with these horizons, we should take $M_A\leq M\leq M_C$, and the values of M_A and M_C depend on the spacetime parameters.

Now we analyze the influence of parameters on $M-r$ curves, and the existence condition of the black hole and cosmological horizons. The Eq. (2.6) implies that when the parameters are chosen as $Q=1,\ \omega=-2/3,\ \alpha=0.01$, to ensure the existence of two horizons in RN-dSQ spacetime the minimum value of the cosmological constant is $l^2=12.7168$, which is shown in Fig. 2a. Namely, there exist both the black hole and cosmological horizons in RN-dSQ spacetime as $l^2>12.7168$. On the other hand, the maximum value of α is 0.1 under the same set of parameters shown in Fig. 2b. That is, when normalization factor associated with the quintessence density of dark energy $\alpha<0.1$, both the black hole and cosmological horizons can survive. From Fig. 2c we can see that the value of ω has no effect on the existence of two horizons. Accordingly, two parameters which have effect on the existence of two horizons are the cosmological constant l^2 and the normalization factor associated with the quintessence density of dark energy α.

Since in the range of $M_A\leq M\leq M_C$ there exists the black hole horizon r_+ in RN-dSQ spacetime, which corresponds to the curve $A-B-C$. And the cosmological horizon r_c corresponds to the curve $C-D-E$. And the points A and C correspond to the minimum and maximum energies of spacetime endow with two horizons, respectively. The cases of $M<M_A$ and $M>M_C$ are not within our consideration, because these two horizons cannot exist together in a RN-dSQ spacetime. When the parameters $Q,\ \omega,\ \alpha$, from Eq. (2.6) are given, we can obtain the relations between the minimum value of cosmological constant (l^2_{min}) and horizon radius under which two horizons can both exist:

$$2Q^2-\frac{6r^4}{l^2_{min}}-3\omega(3\omega+1)\alpha r^{-3\omega+1} =0,\ r^2-Q^2-\frac{3r^4}{l^2_{min}}+3\omega\alpha r^{-3\omega+1}=0. \tag{2.7}$$

For different values of $Q,\ \omega,\ \alpha$, by solving above equations we present the minimum values of the cosmological constant in Table 1.

In addition, from Eq. (2.5) we have

$$r_+\frac{(1-x)}{x}\ -\frac{Q^2(1-x)}{r_+}-\frac{r_+^3(1-x^3)}{l^2x^3} -\alpha r_+^{-3\omega}(x^{3\omega}-1)=0, \tag{2.8}$$

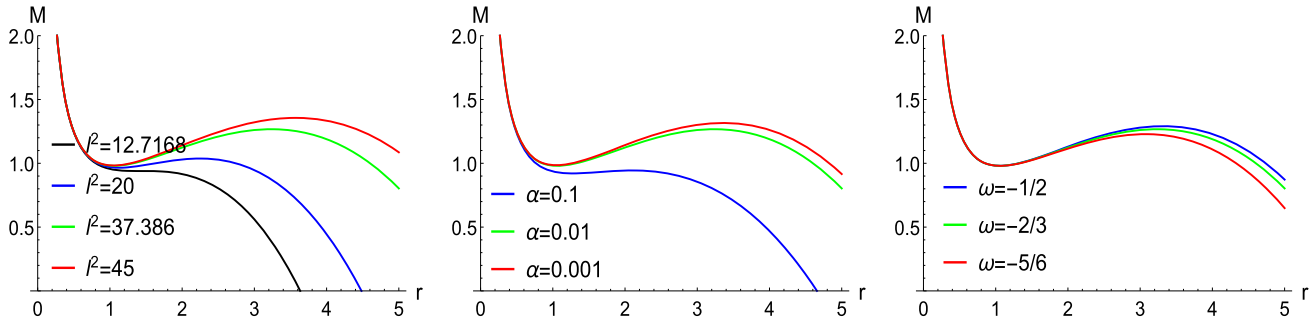

(a) $\omega=-2/3,\ \alpha=0.01$ **(b)** $\omega=-2/3,\ l^2=37.386$ **(c)** $l^2=37.386,\ \alpha=0.01$

Fig. 2 $M-r$ curves with different values of l^2, α, and ω with $Q=1$

Table 1 Minimum values of cosmological constant $l^2_{\min}$ for given other parameters

$\omega=-2/3$	$\alpha=0.1$	$\alpha=0.01$	$\alpha=0.001$
$l^2_{\min}$	26.3171	12.7168	12.0682
$\alpha=0.01$	$\omega=-1/2$	$\omega=-2/3$	$\omega=-5/6$
$l^2_{\min}$	12.4416	12.7168	13.1001

where $x \equiv r_+/r_c$ is ratio between the black hole horizon r_+ and cosmological horizon r_c. At the points A and C, there exists the following equation

$$\frac{1}{2}-\frac{Q^2}{2r_+^2}-\frac{3r_+^2}{2l^2}+\frac{3\omega\alpha}{2}r_+^{-3\omega-1}=0. \tag{2.9}$$

For simplification, we choose

$$\frac{3\alpha}{r_+^{1+3\omega}}=\frac{3\alpha(4\pi r_+^2)}{4\pi r_+^{3+3\omega}}=-\frac{A_+\rho_+}{2\pi\omega}=-\frac{\beta_+}{2\pi\omega}, \tag{2.10}$$

where β_+ is the quintessence field on the black hole horizon. Then Eq. (2.9) can be rewritten as

$$\frac{\beta_+}{2\pi}=\left(1-\frac{Q^2}{r_+^2}-\frac{3r_+^2}{l^2}\right), \tag{2.11}$$

By combining Eqs. (2.8) and (2.9), r_+ can be solved

$$r_+^2=\frac{-b+\sqrt{b^2-4ac}}{2a}, \tag{2.12}$$

where

$$a=-\frac{1}{l^2}\left(\frac{(1-x^3)}{x^3}+\frac{x^{3\omega}}{\omega}(1-x^{-3\omega})\right), \tag{2.13}$$

$$b=\frac{(1-x)}{x}+\frac{x^{3\omega}(1-x^{-3\omega})}{3\omega},$$

$$c=-Q^2\left((1-x)+\frac{x^{3\omega}(1-x^{-3\omega})}{3\omega}\right). \tag{2.14}$$

Using the definition $x_{min}=r_A/r_E$ shown in Fig. 1, we can plot the $x_{min}-l^2$ curves with respect to variant parameters by substituting Eq. (2.12) into Eq. (2.11). And the numerical results of x_{min} for different parameters are shown in Table 2. The results show that the minimum value x_{min} is merely independent of β_+ and l^2, but it is more sensitive to ω, conversely.

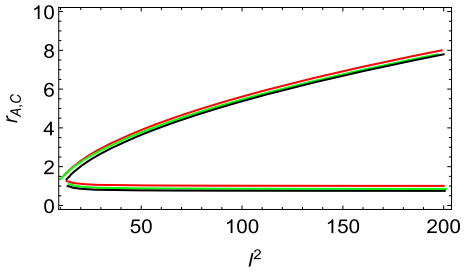

Fig. 3 $r_{A,C}-l^2$ curves with $Q=1$, $\omega=-1/2$. The red solid line stands for $\beta_+=0.0001$, the green solid line for $\beta_+=0.0005$, and the black solid line for $\beta_+=0.0008$

According to Eq. (2.11), one has

$$r^2_{A,C}=l^2\frac{\left(1-\frac{\beta_+}{2\pi}\right)\pm\sqrt{\left(1-\frac{\beta_+}{2\pi}\right)^2-12Q^2/l^2}}{6}. \tag{2.15}$$

The above equation implies that the minimum radius r_A and the maximum radius r_C of black hole horizon position in RN-dSQ spacetime are independent of the value of ω. Taking Q=1, $\beta_+=0.0001, 0.0005, 0.0008$, one can draw the curves of $r_{A,C}-l^2$, where one value of l^2 correspond to two values of r, i.e. r_A and r_C. Therefore, the values of M_A and M_C depend on l^2 once β_+ and Q are fixed. Figure 3 shows that r_C increases with the increase of l^2, while r_A remains nearly unchanged, which is consistent with the fact that x_{min} is independent on l^2.

To study the thermodynamic properties of RN-dSQ spacetime , we need to study the thermodynamic properties of RN-dSQ spacetime endowed with the black hole horizon and the cosmological horizon. While the existence of these two horizons is determined by their position ratio x. The minimum value of x (x_{min}) as the function of l^2 with the quintessence parameter ω and the quintessence field β_+ are exhibited in Fig. 4a and b, respectively. The results show that x_{min} is less affected both by l^2 and β_+, while it is more sensitive to the quintessence parameter ω. Therefore, we adopt $x_{min}\le x\le 1$ as the range of ratio x to study the thermodynamic properties of RN-dSQ spacetime .

Table 2 Minimum values of the ratio between two horizon $x^2_{\min}$ for given other parameters

$\omega=-2/3, l^2_{\min}=37.386$	$\beta_+=0.0001$	$\beta_+=0.0005$	$\beta_+=0.0008$
$x_{\min}$	0.431763	0.431753	0.431746
$\beta_+=0.0005, l^2_{\min}=37.386$	$\omega=-1/2$	$\omega=-2/3$	$\omega=-5/6$
$x^2_{\min}$	0.376711	0.431753	0.480403
$\beta_+=0.0005, \omega=-2/3$	$l^2=20$	$l^2=37.386$	$l^2=45$
$x^2_{\min}$	0.43374	0.431753	0.430163

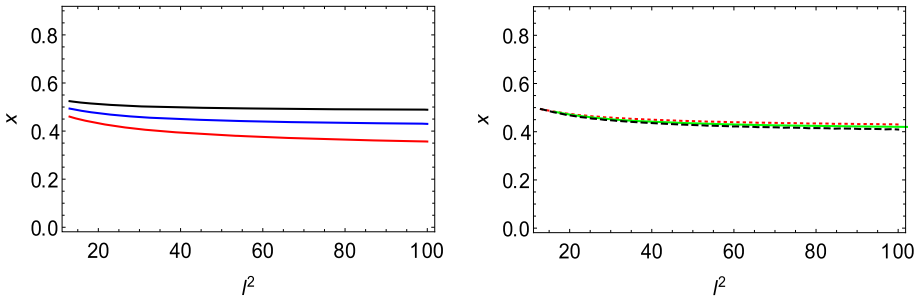

(a) $\beta_+ = 0.0005$ **(b)** $\omega = -1/2$

Fig. 4 Curves of $x_{min} - l^2$ with $Q = 1$. **a** The black solid line stands for $\omega = -1/2$, the blue solid line is for $\omega = -2/3$, and the red solid line is for $\omega = -5/6$. **b** the red dotted line stands for $\beta_+ = 0.0001$, the green solid line is for $\beta_+ = 0.0005$, and the black dashed line is for $\beta_+ = 0.0008$

3 Effective thermodynamic quantities of RN-dSQ spacetime

For the RN-dSQ spacetime, we focus on the space between the black hole and the cosmological horizon. Thus the volume of system reads [48,49]

$$V = \frac{4\pi}{3}\left(r_c^3 - r_+^3\right) = \frac{4\pi}{3x^3} r_+^3 (1 - x^3). \tag{3.1}$$

When introducing the interaction between the two horizons, the total entropy of system is the sum of two individual horizon entropies and their interactive term, which is a function of positions of the two horizons

$$S = \pi r_c^2 (1 + x^2 + f(x)) = \pi r_+^2 (1 + x^2 + f(x))/x^2. \tag{3.2}$$

Here the undefined function $f(x)$ represents the extra contribution from the correlations of two horizons. Based on the first law of black hole thermodynamics:

$$dM = T_{eff} dS - P_{eff} dV + \phi_{eff} dQ \tag{3.3}$$

and Eqs. (3.1), (3.2), and (3.3), the interactive function $f(x)$, effective temperature, and effective pressure of this system have the following forms [59]

$$f(x) = \frac{8}{5}\left(1 - x^3\right)^{2/3} - \frac{2\left(4 - 5x^3 - x^5\right)}{5\left(1 - x^3\right)}, \tag{3.4}$$

$$T_{eff} f_1(x) - \frac{f_2(x)}{r_+} + Q^2 \frac{f_3(x)}{r_+^3} = 0, \tag{3.5}$$

$$P_{eff} F_1(x) r_+^4 + F_2(x) r_+^2 + F_3(x) = 0 \tag{3.6}$$

with

$$f_1(x) = \frac{4\pi(1 + x^4)}{1 - x},$$

$$f_3(x) = (1 + x + x^2)(1 + x^4) - 2x^3,$$

$$F_1(x) = \frac{8\pi(1 + x^4)}{x(1 - x)},$$

$$f_2(x) = (1 + x)(1 + x^3) - 2x^2 - \frac{\beta_+ x^{3+3\omega}}{2\pi\omega(1 - x)}\left[1 - x^{-3\omega} - \omega(x^3 - x^{-3-3\omega})\right],$$

$$F_2(x) = \left(x(1 + x) + \frac{\beta_+ x^{4+3\omega}(1 - x^{3-3\omega})}{2\pi(1 - x)}\right)(x + f'(x)/2) - \left(\frac{(1 + 2x)}{(1 + x + x^2)} - \frac{\beta_+ x^3 (x^{2\omega} - (2 - \omega)x^5 + (1 - \omega)x^8)}{2\pi\omega(1 - x^3)(1 - x)}\right)(1 + x^2 + f(x)),$$

$$F_3(x) = Q^2\left(\frac{(1 + 2x + 3x^2)}{(1 + x + x^2)}(1 + x^2 + f(x)) - (1 + x + x^2 + x^3)(x + f'(x)/2)\right).$$

For the given effective temperature T_{eff}, from Eq. (3.5) the inverse of black hole horizon radius satisfies

$$\frac{1}{r_+} = 2\sqrt{\frac{f_2(x)}{3Q^2 f_3(x)}}\cos(\theta + 120^0). \tag{3.7}$$

Once P_{eff} is given, r_+^2 satisfies the following equation according to Eq. (3.5)

$$r_+^2 = \frac{-F_2(x) + \sqrt{F_2^2(x) - 4P_{eff} F_1(x) F_3(x)}}{2P_{eff} F_1(x)}. \tag{3.8}$$

In order to further understand the effective temperature of this system, we should compare it with the temperatures on two horizons. From Eq. (2.5) we can obtain the Hawking temperatures of the black hole and the cosmological horizons as follows:

$$T_+ = \frac{1}{4\pi r_+}\left(1 - \frac{Q^2}{r_+^2} - \frac{3r_+^2}{l^2} - \frac{\beta_+}{2\pi}\right), \tag{3.9}$$

$$T_c = -\frac{x}{4\pi r_+}\left(1 - \frac{Q^2 x^2}{r_+^2} - \frac{3r_+^2}{x^2 l^2} - \frac{\beta_+}{2\pi} x^{1+3\omega}\right) \tag{3.10}$$

with

$$r_+^2 = \frac{x^2}{(1 + x + x^2)} \frac{1 \pm \sqrt{1 - \frac{4Q^2(1+x+x^2)}{x}\left(\frac{1}{l^2} - \frac{\beta_+(1-x^{-3\omega})x^{3+3\omega}}{6\pi\omega(1-x^3)}\right)}}{2\left(\frac{1}{l^2} - \frac{\beta_+(1-x^{-3\omega})x^{3+3\omega}}{6\pi\omega(1-x^3)}\right)}. \tag{3.11}$$

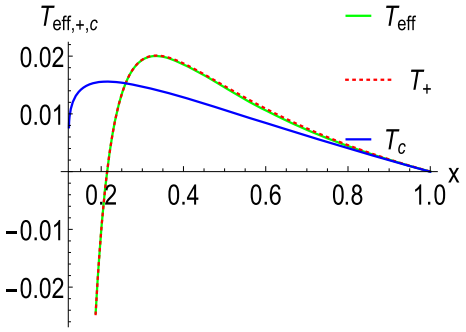

Fig. 5 Lines show T_{eff}, T_+ and T_c as a function of x

Substituting Eq. (3.11) into Eq. (3.5), (3.9) and (3.10), we plot the curves with the parameters $Q = 1$, $\omega = -2/3$, $\beta_+ = 0.0005$, $l^2 = 37.386$ in Fig. 5.

It is obviously that the trends of T_{eff} and T_+ with respect to x are same for the fixed parameters Q, ω, β_+, and l^2. This implies the effective temperature can be replaced with the one on black hole horizon. In addition, the influence of parameters on the effective temperature is exhibited in Fig. 6, from which we can see that the behavior of temperature as a function of x is merely independent of ω and β_+ when l^2 is given. However, for the fixed parameters Q, ω, and β_+, the behavior of T_{eff} with respect to x is only affected by l^2.

4 phase transition of RN-dSQ spacetime

In this section, we would like to study the phase transition in the canonical ensemble. The Gibbs free energy of RN-dSQ spacetime reads

$$\begin{aligned} G(r_+,x) &= \frac{r_+(1+x)}{2(1+x+x^2)} \\ &+\frac{Q^2(1+x)(1+x^2)}{2r_+(1+x+x^2)}+\frac{r_+(1-x)D(x,\omega)}{6x^3(1+x^4)}(1-x^3) \\ &+\beta_+ r_+ x\frac{x^{3\omega}[(1+x)(1-x^3)-2x^2]+(1+x)(1-x^2)}{12\pi\omega(1+x+x^2)(1-x^3)} \\ &-\frac{r_+(1-x)}{4x^2(1+x^4)}(1+x^2+f_0(x))\Big\{\Big[(1+x)(1+x^3)-2x^2\Big] \\ &-\frac{Q^2}{r_+^2}\Big[(1+x+x^2)(1+x^4)-2x^3\Big] \\ &-\frac{\beta_+ x^{3+3\omega}}{2\pi\omega(1-x)}\Big[1-x^{-3\omega}-\omega(x^3-x^{-3-3\omega})\Big]\Big\}. \end{aligned} \tag{4.1}$$

The critical point denotes a second-order phase transition which is determined by the following equations

$$\left(\frac{\partial P_{eff}}{\partial V}\right)_{T_{eff},Q,\beta_+,\omega} = \left(\frac{\partial^2 P_{eff}}{\partial V^2}\right)_{T_{eff},Q,\beta_+,\omega} = 0. \tag{4.2}$$

According to Eq. (4.2), when choosing $Q = 1, \beta_+ = 0.0005$, $\omega = -1/2$, one obtains the critical point of spacetime as

$$\begin{aligned} &r_+^c = 2.64432,\ x^c = 0.656434, \\ &V^c = 0.0253530\frac{4\pi(r_+^c)^3}{3} = 1.96363483 \\ &T_{eff}^c = \frac{0.2869}{4\pi r_+^c} = 0.00863395, \quad P_{eff} = \frac{0.10257633}{8\pi(r_+^c)^2} \\ &\quad = 0.000583686. \end{aligned}$$

Substituting Eq. (3.7) into Eqs. (3.1) and (3.6), we plot the isothermal curves of $P_{eff} - V$ in Fig. 7. It shows that the value of ω has no effect on the isothermal curve of $P_{eff} - V$, while the curve of $P_{eff} - V$ is more sensitive to the parameter β_+.

It is shown in Fig. 7a that the isotherm of equation of state is in the range of $P_{eff}^{min} < P_{eff} < P_{eff}^{max}$, there are three possible values of V which correspond to the same value of P_{eff}. Furthermore, for the range of $P_{eff}^{min} < P_{eff} < P_{eff}^{max}$, the slope of curve is positive, i.e., $\left(\frac{\partial P_{eff}}{\partial V}\right)_{T_{eff},Q} > 0$, which does not meet the condition of stable equilibrium. Therefore, those states are impossible to achieve as homogeneous systems. And the isotherm curves in the range of $P_{eff}^{min} < P_{eff} < P_{eff}^{max}$ are replaced with a straight line, so the areas enclosed by curve and straight are equivalent, that is the Maxwell's equal area law. With the increasing of the effective temperature, these two areas decrease. Until two areas tend to zero, three intersection points of the straight line and the curve tend to one point, which is the critical point. The position of this critical point satisfies Eq. (4.2).

Substituting Eq. (3.7) into Eqs. (3.6) and (4.1), we plot the isotherm curve of $G - P_{eff}$ in Fig. 8.

The results show that when $T_{eff} > T_{eff}^c$, the isotherm curve $G - P_{eff}$ is monotonic. Namely, the RN-dSQ spacetime is in a single state, which corresponds to the gas phase of VdW system. When $T_{eff} < T_{eff}^c$, there exists a point of intersection in $G - P_{eff}$ curve,where the first-order phase transition occurs.

The isobaric heat capacity of spacetime is

$$C_{P_{eff},Q} = T_{eff}\frac{\frac{\partial S}{\partial x}\frac{\partial P_{eff}}{\partial r_+} - \frac{\partial S}{\partial r_+}\frac{\partial P_{eff}}{\partial x}}{\frac{\partial T_{eff}}{\partial x}\frac{\partial P_{eff}}{\partial r_+} - \frac{\partial T_{eff}}{\partial r_+}\frac{\partial P_{eff}}{\partial x}}. \tag{4.3}$$

Substituting Eq. (3.8) into Eqs. (3.5) and (4.3), we have the isobaric curve of $C_{P_{eff}} - T_{eff}$ in Fig. 9a. The volume expansion coefficient reads

$$\beta = \frac{1}{V}\frac{\frac{\partial V}{\partial x}\frac{\partial P_{eff}}{\partial r_+} - \frac{\partial V}{\partial r_+}\frac{\partial P_{eff}}{\partial x}}{\frac{\partial T_{eff}}{\partial x}\frac{\partial P_{eff}}{\partial r_+} - \frac{\partial T_{eff}}{\partial r_+}\frac{\partial P_{eff}}{\partial x}}. \tag{4.4}$$

Then substituting Eq. (3.8) into Eqs. (3.5) and (4.4), we plot the isobaric curve of $\beta - T_{eff}$ in Fig. 9b. The isothermal compression coefficient becomes

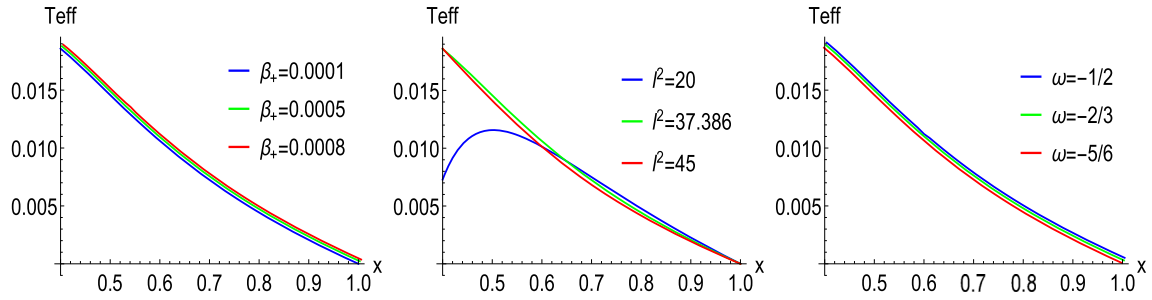

(a) $\omega = -2/3,\ l^2 = 37.386$ **(b)** $\omega = -2/3,\ \beta_+ = 0.0005$ **(c)** $l^2 = 37.386,\ \beta_+ = 0.0005$

Fig. 6 $T_{eff} - x$ curves with $Q = 1$

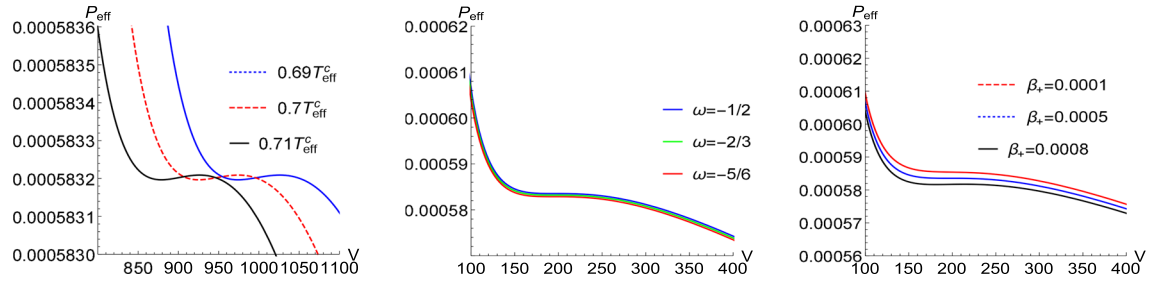

(a) $\omega = -1/2,\ \beta_+ = 0.0005$ **(b)** $\beta_+ = 0.0005,\ \ T_{eff} = T^c_{eff}$ **(c)** $\omega = -1/2,\ \ T_{eff} = T^c_{eff}$

Fig. 7 $P_{eff} - V$ curves for $Q = 1$

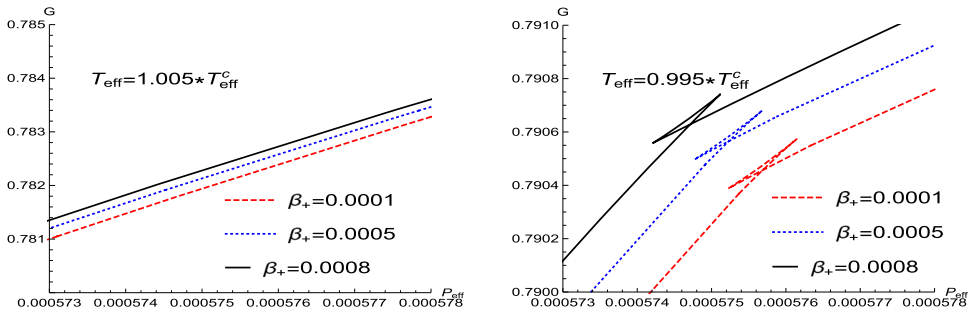

(a) $Q = 1,\ \omega = -1/2$ **(b)** $Q = 1,\ \omega = -1/2$

Fig. 8 $G - P_{eff}$ curves with different values of β_+

$$\kappa_{T_{eff}} = \frac{1}{V}\frac{\frac{\partial V}{\partial x}\frac{\partial T_{eff}}{\partial r_+} - \frac{\partial V}{\partial r_+}\frac{\partial T_{eff}}{\partial x}}{\frac{\partial T_{eff}}{\partial x}\frac{\partial P_{eff}}{\partial r_+} - \frac{\partial T_{eff}}{\partial r_+}\frac{\partial P_{eff}}{\partial x}}. \tag{4.5}$$

Substituting Eq. (3.7) into Eqs. (3.6) and (4.5), we plot the isothermal curve of $\kappa_{T_{eff}} - P_{eff}$ in Fig. 9c. Figure 9 shows that RN-dSQ spacetime presents typical continuous phase transition characteristics, i.e., it possesses the phase transition characteristics of VdW system or AdS black holes. These curves also reflect the influence of parameter β_+ on the critical point.

The isochoric heat capacity of spacetime is

$$C_{V,Q} = T_{eff}\left(\frac{\partial S}{\partial T_{eff}}\right)_{V,Q} = T_{eff}\frac{\frac{\partial S}{\partial x}\frac{\partial V}{\partial r_+} - \frac{\partial S}{\partial r_+}\frac{\partial V}{\partial x}}{\frac{\partial T_{eff}}{\partial x}\frac{\partial V}{\partial r_+} - \frac{\partial T_{eff}}{\partial r_+}\frac{\partial V}{\partial x}}. \tag{4.6}$$

Substituting Eq. (3.1) into Eqs. (3.5) and (4.6), we present the isochoric curve of $C_{V,Q} - T_{eff}$ in Fig. 10.

It can be seen from Fig. 10 that the isochoric heat capacity of spacetime doesn't vanish, which is consistent with the result in Ref. [65,66]. That is different with AdS black holes, whose isochoric heat capacities are zero [33–36]. For any thermodynamic systems, the isochoric heat capacity doesn't vanish in general, so our conclusion is more universal. Therefore, when considering the interaction of two horizons for the RN-dSQ spacetime, the effective thermodynamic quantities and corresponding equations are more closer to the characteristics of an ordinary thermodynamic system. Thus this thermodynamic system described by the effective thermodynamic quantities is more universal.

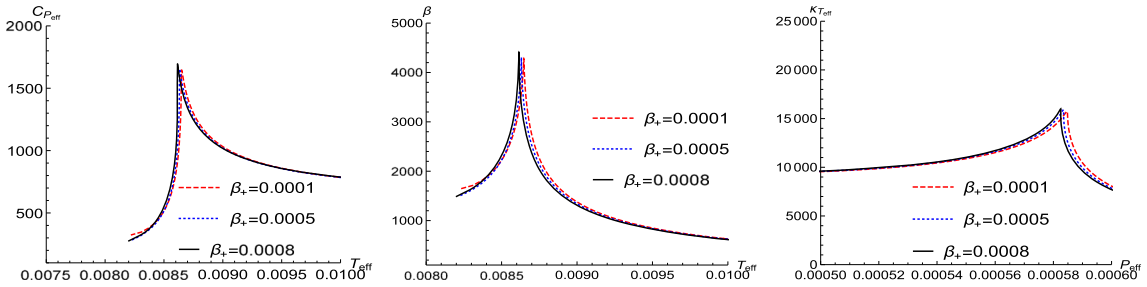

(a) $Q = 1,\ \omega = -1/2$ **(b)** $Q = 1,\ \omega = -1/2$ **(c)** $Q = 1,\ \omega = -1/2$

Fig. 9 Curves of $C_{P_{eff}} - T_{eff}$, $\beta - T_{eff}$, and $\kappa_{T_{eff}} - P_{eff}$ with different values of β_+

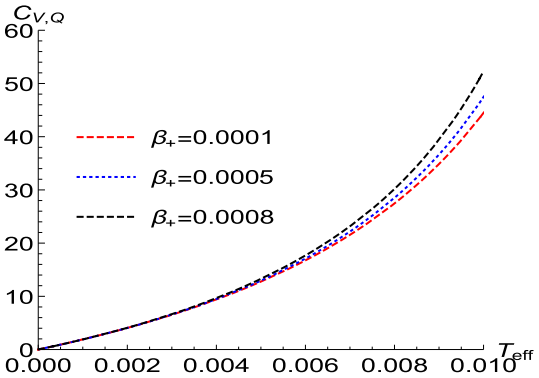

Fig. 10 $C_{V,Q} - T_{eff}$ with different values of β_+ for $Q = 1, \omega = 1/2$

According to Ehrenfest's classification of phase transitions, if the Gibbs functions of two phases and their first-order partial derivatives are continuous, but their second-order partial derivatives are of sudden changes, the phase transition is called the second-order one. From the above analysis, we know that for the lower effective temperature ($T_{eff} < T^c_{eff}$), the entropy and volume will undergo sudden changes, and the spacetime undergoes a first-order phase transition. As $T_{eff} = T^c_{eff}$, the entropy and volume are continuous, while the isobaric heat capacity, isobaric expansion coefficient, and isothermal compression coefficient both have a peak at the critical point shown in Fig. 9.

5 Entropic force between two horizons

The recent exploration of the interactive force between microscopic particles inside black holes has attracted widespread attention [33,67,68]. In order to understand the microstructure of RN-dSQ spacetime more clearly, we will check out the behavior of entropic force between two horizons in this section. The entropic force in a thermodynamic system can be defined as follows [69,70]

$$F = -T\frac{\partial S}{\partial r}, \tag{5.1}$$

where T is the temperature and r is the radius of system. In this part we pay attention on the entropic force between the black hole and cosmological horizons. According to Eq. (3.2), the interactive entropy caused by two horizons reads

$$\tilde{S} = \pi r_c^2 f(x). \tag{5.2}$$

Based on Eq. (5.1), we can introduce the corresponding entropic force between two horizons in the RN-dSQ spacetime

$$\tilde{F} = T_{eff}\left(\frac{\partial \tilde{S}}{\partial r}\right)_{T_{eff}}, \tag{5.3}$$

where T_{eff} stands for the effective temperature of this system and $r \equiv r_c - r_+$. From the above equation, we have

$$\tilde{F}(x) = T_{eff}x^2\frac{\left(\frac{\partial \tilde{S}}{\partial r_+}\right)_x\left(\frac{\partial T_{eff}}{\partial x}\right)_{r_+} - \left(\frac{\partial \tilde{S}}{\partial x}\right)_{r_+}\left(\frac{\partial T_{eff}}{\partial r_+}\right)_x}{x(1-x)\left(\frac{\partial T_{eff}}{\partial x}\right)_{r_+} + r_+\left(\frac{\partial T_{eff}}{\partial r_+}\right)_x}. \tag{5.4}$$

Then substituting Eq. (3.5) into Eqs. (4.2) and (5.4), we can get the $\tilde{F}(x) - x$ curves as shown in Fig. 11.

It is obviously that the entropic force between two horizons depends on the cosmological constant l^2, while merely independent of other parameters β_+ and ω. For the far distance between two horizons (i.e., the small value of x), the entropy force is negative, which indicates there exists an attractive force between two horizons to make them more closer. Up to the certain distance (i.e., the certain value of x), the entropic force is zero. Continuously decreasing the distance, the interactive entropy force between two horizons becomes positive, and it will approach to infinity when two horizons coincide. In the case of $x = 1$, the infinite entropic force prompts them to accelerated separate.

6 Conclusion and discussion

In this work, we introduced the interaction between the black hole and cosmological horizons and presented the effective thermodynamic quantities of the RN-dSQ spacetime.

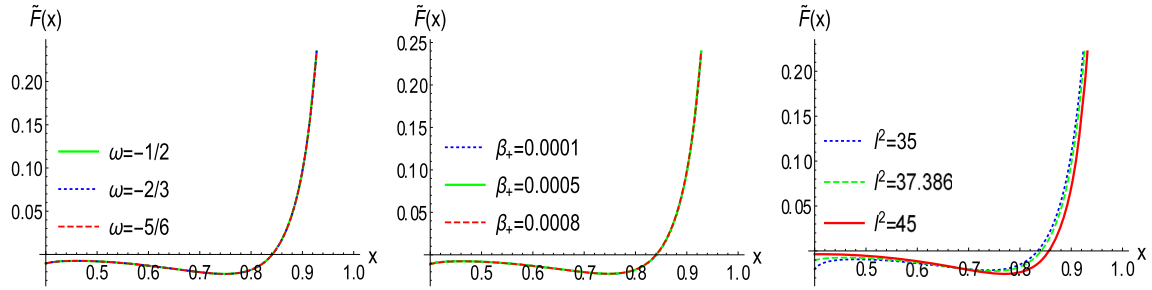

(a) $l^2 = 37.386,\ \beta_+ = 0.0005$ **(b)** $\omega = -2/3,\ l^2 = 37.386$ **(c)** $\omega = -2/3,\ \beta_+ = 0.0005$

Fig. 11 Curves of $\tilde{F}(x) - x$ with $Q = 1$

The related thermodynamical properties of system were also investigated. Through the analysis in Section IV, we know that the RN-dSQ spacetime also have the continuous phase transitions and first-order ones, that is similar to VdW system or AdS black holes. The results showed that the effective temperature and phase transition point are independent of the RN-dSQ spacetime quintessence dark energy barotropic index ω. The existence of the black hole and cosmological horizons are determined by the cosmological constant and the normalization factor associated with the quintessence density of dark energy α when other parameters are given. Based on the effective quantities of system, we found that the isochoric heat capacity is non-zero, and it increases with the effective temperature and quintessence field β_+. This conclusion is similar to ordinary thermodynamic systems, so our results have more general physical meanings.

From the curve of $\tilde{F}(x) - x$, the characteristic of the change of entropic force with x is: when $x \to 1$, the entropic force tends to infinity, which indicates that the infinite entropic force leads to accelerated separation between two horizons. At the same time, two horizons will be accelerating separation under the infinity entropic force, and the energy M of system will decrease. Continuously decreasing the value of x, the entropic force will become negative and prevent the separation of two horizons. On the other hand, from the curve $T_{eff} - x$ we found that for the low effective temperature (i.e., the large value of x), the entropic force between the two horizons promotes the separation of two horizons. While for the high effective temperature (i.e., the small value of x), the entropic force prevents the separation of the two horizons. These conclusions will provide a theoretical foundation for studying the evolution of spacetime.

In addition, comparing the entropic force between two horizons with the Lennard–Jones force between two particles, we found the curves obtained by completely different methods for different systems are so surprisingly similar. The Lennard–Jones force of two particles is inherently related to the entropic force between two horizons. To further study the thermodynamic properties of black holes, it is necessary to explore the microstructure of system. We had shown the interactive force between two horizons, which reflected the interactive force between microscopic particles on the curved surfaces (the black hole and cosmological horizons) in dS spacetime. The method can be extended to study the interaction of microscopic particles inside black holes, which will provides a new way to explore the interaction between black hole molecules.

Acknowledgements We thank Prof. M. S. Ma and Prof. Z. H. Zhu for useful discussions.
This work was supported by the National Natural Science Foundation of China (Grant Nos. 12075143, 11971277), the Scientific and Technological Innovation Programs of Higher Education Institutions of Shanxi Province, China (Grant no. 2020L0471, no. 2020L0472) and the Science Technology Plan Project of Datong City, China (Grant no. 2020153).

Data Availability Statement This manuscript has no associated data or the data will not be deposited. [Authors' comment: In our work, there is no experimental data, just has the numerical calculated data obtained from the theoretical analyze. The numerical calculated data that support the findings of this study are openly available.]

Funded by SCOAP^3. SCOAP^3 supports the goals of the International Year of Basic Sciences for Sustainable Development.

References

1. LIGO Collaboration and Virgo Collaboration, Observation of gravitational waves from a binary black hole merger. Phys. Rev. Lett. **116**, 061102 (2016). arXiv:1602.03837

2. EHT Collaboration, First m87 event horizon telescope results. I. the shadow of the supermassive black hole. Astrophys. J. Lett. **875**, L1 (2019). arXiv:1906.11238
3. EHT Collaboration, First m87 event horizon telescope results. II. array and instrumentation. Astrophys. J. Lett. **875**, L2 (2019). arXiv:1906.11239
4. EHT Collaboration, First m87 event horizon telescope results. III. data processing and calibration. Astrophys. J. Lett. **875**, L3 (2019). arXiv:1906.11240
5. EHT Collaboration, First m87 event horizon telescope results. IV. imaging the central supermassive black hole. Astrophys. J. Lett. **875**, L4 (2019). arXiv:1906.11241
6. EHT Collaboration, First m87 event horizon telescope results. V. physical origin of the asymmetric ring. Astrophys. J. Lett. **875**, L5 (2019). arXiv:1906.11242
7. EHT Collaboration, First m87 event horizon telescope results. VI. the shadow and mass of the central black hole. Astrophys. J. Lett. **875**, L6 (2019). arXiv:1906.11243
8. S.W. Hawking, Particle creation by black holes. Commun. Math. Phys. **43**, 199–220 (1975)
9. J.D. Bekenstein, Black holes and entropy. Phys. Rev. D **7**, 2333–2346 (1973)
10. J.M. Bardeen, B. Carter, S.W. Hawking, The four laws of black hole mechanics. Commun. Math. Phys. **31**, 161–170 (1973)
11. S.W. Hawking, D.N. Page, Thermodynamics of black holes in Anti-de Sitter space. Commun. Math. Phys. **87**, 577–588 (1983)
12. K. David, R.B. Mann, P-V criticality of charged AdS black holes. JHEP **07**, 033 (2012)
13. R.G. Cai, L.M. Cao, L. Li, R.Q. Yang, P-V criticality in the extended phase space of Gauss–Bonnet black holes in AdS space. JHEP **09**, 005 (2013)
14. S. Gunasekaran, D. Kubiznak, R.B. Mann, Extended phase space thermodynamics for charged and rotating black holes and Born–Infeld vacuum polarization. JHEP **11**, 110 (2012)
15. A.M. Frassino, D. Kubiznak, R.B. Mann, F. Simovic, Multiple reentrant phase transitions and triple points in lovelock thermodynamics. JHEP **09**, 080 (2014)
16. J.D. Bairagya, K. Pal, K. Pal, T. Sarkar, The geometry of RN-AdS fluids. Phys. Lett. B **805**, 135416 (2020)
17. R.G. Cai, S.M. Ruan, S.J. Wang, R.Q. Yang, R.H. Peng, Complexity growth for AdS black holes. JHEP **09**, 161 (2016)
18. J.L. Zhang, R.G. Cai, H.W. Yu, Phase transition and thermodynamical geometry of Reissner–Nordström-AdS Black holes in extended phase space. Phys. Rev. D **91**, 044028 (2015)
19. S.H. Hendi, R.B. Mann, S. Panahiyan, B.E. Panah, Van der Waals like behavior of topological AdS black holes in massive gravity. Phys. Rev. D **95**, 021501(R) (2017)
20. A. Dehghani, S.H. Hendi, R.B. Mann, Range of novel black hole phase transitions via massive gravity: triple points and N-fold reentrant phase transitions. Phys. Rev. D **101**, 084026 (2020)
21. H. Ranjbari, M. Sadeghi, M. Ghanaatian, G. Forozani, Critical behavior of AdS Gauss–Bonnet massive black holes in the presence of external string cloud. Eur. Phys. J. C **80**, 17 (2020)
22. M. Chabab, H. El Moumni, S. Iraoui, K. Masmar, Phase transitions and geothermodynamics of black holes in dRGT massive gravity. Eur. Phys. J. C **79**, 342 (2019)
23. S.Z. Han, J. Jiang, M. Zhang, W.B. Liu, Photon sphere and phase transition of d-dimensional ($d \geq 5$) charged Gauss–Bonnet AdS black holes. Commun. Theor. Phys. **72**, 10 (2020)
24. A. Dehyadegari, A. Sheykhi, Critical behavior of charged dilaton black holes in AdS space. Phys. Rev. D **102**, 064021 (2020)
25. D. Mago, N. Breton, Thermodynamics of the Euler–Heisenberg-AdS black hole. Phys. Rev. D **102**, 084011 (2020)
26. S.N. Sajadi, N. Riazi, S.H. Hendi, Dynamical and thermal stabilities of nonlinearly charged AdS black holes. Eur. Phys. J. C **79**, 775 (2019)
27. S.H. Hendi, A. Dehghani, Criticality and extended phase space thermodynamics of AdS black holes in higher curvature massive gravity. Eur. Phys. J. C **79**, 227 (2019)
28. S. Guo, E.W. Liang, Ehrenfest's scheme and microstructure for regular-AdS black hole in the extended phase space. Class. Quantum Gravity **38**, 125001 (2021)
29. S.H. Hendi, K. Jafarzade, Critical behavior of charged AdS black holes surrounded by quintessence via an alternative phase space. Phys. Rev. D **103**, 104011 (2021)
30. Z.M. Xu, Analytic phase structures and thermodynamic curvature for the charged AdS black hole in alternative phase space. Front. Phys. **16**, 24502 (2021)
31. Y.C. Huang, H.M. Jing, J. Tao, F.Y. Yao, Phase structures and transitions of quintessence surrounding RN Black holes in a grand canonical ensemble. Chin. Phys. C **45**, 075101 (2021)
32. A. Dehyadegari, A. Sheykhi, A. Montakhab, Critical behaviour and microscopic structure of charged AdS black holes via an alternative phase space. Phys. Lett. B **768**, 235–240 (2017)
33. S.W. Wei, Y.X. Liu, R.B. Mann, Repulsive interactions and universal properties of charged anti-de Sitter black hole microstructures. Phys. Rev. Lett. **123**, 071103 (2019)
34. S.W. Wei, Y.X. Liu, Extended thermodynamics and microstructures of four-dimensional charged Gauss–Bonnet black hole in AdS space. Phys. Rev. D **101**, 104018 (2020)
35. R. Zhou, Y.X. Liu, S.W. Wei, Phase transition and microstructures of five-dimensional charged Gauss–Bonnet-AdS black holes in the grand canonical ensemble. Phys. Rev. D **102**, 124015 (2020). arXiv:2008.08301
36. S.W. Wei, Y.X. Liu, Intriguing microstructures of five-dimensional neutral Gauss–Bonnet AdS black hole. Phys. Lett. B **803**, 135287 (2020)
37. Y.G. Miao, Z.M. Xu, On thermal molecular potential among micromolecules in charged AdS black hole. Phys. Rev. D **98**, 044001 (2018)
38. Y.G. Miao, Z.M. Xu, Microscopic structures and thermal stability of black holes conformally coupled to scalar fields. Nucl. Phys. B **942**, 205–220 (2019)
39. X.Y. Guo, H.F. Li, L.C. Zhang, R. Zhao, Continuous phase transition and microstructure of charged AdS black hole with quintessence. Eur. Phys. J. C **80**, 168 (2020)
40. X.Y. Guo, H.F. Li, L.C. Zhang, R. Zhao, Microstructure and continuous phase transition of RN-AdS black hole. Phys. Rev. D **100**, 064036 (2019)
41. G.A. Marks, F. Simovic, R.B. Mann, Phase transitions in 4D Gauss–Bonnet-de Sitter black holes. arXiv:2107.11352v1
42. G.E. Volovik, Effect of the inner horizon on the black hole thermodynamics: Reissner–Nordström black hole and Kerr black hole. arXiv:2107.11193
43. R.G. Cai, Cardy–Verlinde formula and thermodynamics of black holes in de Sitter spaces. Nucl. Phys. B **628**, 375–386 (2002)
44. Y. Sekiwa, Thermodynamics of de Sitter black holes: thermal cosmological constant. Phys. Rev. D **73**, 084009 (2006)
45. M. Urano, A. Tomimatsu, H. Saida, Mechanical first law of black hole spacetimes with cosmological constant and its application to Schwarzschild-de Sitter spacetime. Class. Quantum Gravity **26**, 105010 (2009)
46. S. Mbarek, R.B. Mann, Reverse Hawking-Page phase transition in de Sitter black holes. JHEP **02**, 103 (2019)
47. D. Kubiznak, F. Simovic, Thermodynamics of horizons: de Sitter black holes and reentrant phase transitions. Class. Quantum Gravity **33**, 245001 (2016)
48. F. Simovic, R.B. Mann, Critical phenomena of Born–Infeld-de Sitter black holes in cavities. JHEP **05**, 136 (2019)
49. S. Haroon, R.A. Hennigar, R.B. Mann, F. Simovic, Thermodynamics of Gauss–Bonnet-de Sitter black holes. Phys. Rev. D **101**, 084051 (2020)

50. F. Simovic, D. Fusco, R.B. Mann, Thermodynamics of de Sitter black holes with conformally coupled scalar fields. arXiv:2008.07593 [gr-qc]
51. M. Chabab, H. El Moumni, J. Khalloufi, On Einstein-non linear-Maxwell–Yukawa de-Sitter black hole thermodynamics. arXiv:2001.01134 [hep-th]
52. B.P. Dolan, D. Kastor, D. Kubiznak, R.B. Mann, J. Traschen, Thermodynamic volumes and isoperimetric inequalities for de Sitter black holes. Phys. Rev. D **87**, 104017 (2013)
53. S. Bhattacharya, A note on entropy of de Sitter black holes. Eur. Phys. J. C **76**, 112 (2016)
54. J. McInerney, G. Satishchandrana, J. Traschena, Cosmography of KNdS Black holes and isentropic phase transitions. Class. Quantum Gravity **33**, 105007 (2016)
55. P. Kanti, T. Pappas, Effective temperatures and radiation spectra for a higher-dimensional Schwarzschild-de-Sitter black-hole. Phys. Rev. D **96**, 024038 (2017)
56. L.J. Romans, Supersymmetric, cold and lukewarm black holes in cosmological Einstein–Maxwell theory. Nucl. Phys. B **383**, 395–415 (1992)
57. Y.B. Ma, Y. Zhang, L.C. Zhang, L. Wu, Y.M. Huang, Y. Pan, Thermodynamic properties of higher-dimensional dS black holes in dRGT massive gravity. Eur. Phys. J. C **80**, 213 (2020)
58. X.Y. Guo, H.F. Li, L.C. Zhang, R. Zhao, Entropy of higher dimensional charged Gauss–Bonnet black hole in de Sitter Space. Commun. Theor. Phys. **72**, 085403 (2020)
59. F. Liu, L.C. Zhang, On thermodynamics of RN-dS black hole surrounded by the quintessence. Chin. J. Phys. **57**, 53–60 (2019)
60. J. Dinsmore, P. Draper, D. Kastor, Y. Qiu, J. Traschen, Schottky anomaly of de Sitter black holes. Class. Quantum Gravity **37**, 054001 (2020)
61. C.V. Johnson, Specific heats and Schottky peaks for black holes in extended thermodynamics. Class. Quantum Gravity **37**, 054003 (2020)
62. V.V. Kiselev, Quintessence and black holes. Class. Quantum Gravity **20**, 1187 (2003)
63. H. Liu, X.H. Meng, Effects of dark energy on the efficiency of charged AdS black holes as heat engine. Eur. Phys. J. C **77**, 556 (2017)
64. C.H. Nama, Non-linear charged dS black hole and its thermodynamics and phase transitions. Eur. Phys. J. C **78**, 418 (2018)
65. J. Dinsmore, P. Draper, D. Kastor, Y. Qiu, J. Traschen, Schottky anomaly of deSitter black holes. Class. Quantum Gravity **37**, 054001 (2020)
66. C.V. Johnson, Specific heats and Schottky peaks for black holes in extended thermodynamics. Class. Quantum Gravity **37**, 054003 (2020)
67. S.W. Wei, Y.X. Liu, R.B. Mann, Characteristic interaction potential of black hole molecules from the microscopic interpretation of Ruppeiner geometry. arXiv:2108.07655 [gr-qc]
68. S. Dutta, G.S. Punia, On the interaction between AdS black hole molecules. arXiv:2108.06135 [hep-th]
69. H.H. Zhao, L.C. Zhang, Y. Gao, F. Liu, Entropic force between two horizons of dilaton black holes with a power-Maxwell field. Chin. Phys. C **45**, 043111 (2021)
70. E. Verlinde, On the origin of gravity and the laws of Newton. JHEP **1104**, 029 (2011)